Article:
Qian, K orcid.org/0000-0002-8719-1537, Li, Z, Zhang, Z orcid.org/0000-0003-0204-3867 et al. (1 more author) (2023) Data-driven Adaptive Iterative Learning Control of a Compliant Rehabilitation Robot for Repetitive Ankle Training. IEEE Robotics and Automation Letters, 8 (2). pp. 656-663. ISSN 2377-3766

https://doi.org/10.1109/LRA.2022.3229570

Data-driven Adaptive Iterative Learning Control of a Compliant Rehabilitation Robot for Repetitive Ankle Training

Kun Qian, Zhenhong Li, Zhiqiang Zhang, *Member, IEEE,*, Guqiang Li, and Sheng Q. Xie, *Senior Member, IEEE*

***Abstract*—This paper investigates the repetitive range of motion (ROM) training control for a compliant ankle rehabilitation robot (CARR). The CARR utilizes four pneumatic muscle (PM) actuators to manipulate the ankle with three rational degree-of-freedoms (DoFs) and soft human-robot interaction, but the strong-nonlinearity of the PM actuator makes precise tracking difficult. To improve the training effectiveness, a data-driven adaptive iterative learning controller (DDAILC) is proposed based on compact form dynamic linearization (CFDL) with estimated pseudo-partial derivative (PPD). Instead of using a PM dynamic model, the estimated PPD is updated merely by online input-output (I/O) measures. Sufficient conditions are established to guarantee the convergence of tracking errors and the boundedness of control input. Experimental studies are conducted on ten human participants with two therapist-resembled trajectories. Compared with other data-driven methods, the proposed DDAILC demonstrates significant improvement on tracking performance.**

***Index Terms*—Ankle rehabilitation robot, pneumatic muscle, iterative learning control, adaptive control.**

I. Introduction

INTENSIVE ankle passive stretching is widely utilized in the treatment of limited ankle range of motion (ROM) for traumatic head injury and stroke patients [1]. To ease the great burden of therapists, a range of platform-based ankle rehabilitation robots are developed for passive training purposes, e.g., ARBOT [2] and Rutgers ankle [3]. However, existing platform-based robots have inconsistent rotation center with the ankle joint which discounts the recovery performance [4]. Meanwhile, a large proportion of existing devices employ non-backdrivable rigid actuators, e.g., electric motors and cylinders, which causes non-compliant human-robot interaction [5].

To overcome aforementioned limitations, a compliant ankle rehabilitation robot (CARR) was developed by our group [6]. The CARR employs a parallel structure to achieve three rotational degrees-of-freedoms (DoFs) where the required torque is actuated above the end effector with fixed rotation center. Pneumatic muscle (PM) actuators are soft, light weight and able to generate large force with short contraction. However, PM actuators exhibit highly nonlinear dynamics, which cause difficulties in dynamic modeling and controller design for precise tracking [6–8]. Since the outcomes of ankle passive training largely rely on the completion of the ROM trajectory suggested by the therapist [9]. Therefore, it is essential to improve the trajectory tracking accuracy of the CARR under passive training scenarios.

Various tracking control methods have been developed for the existing platform-based ankle robots. A torque-based velocity controller was proposed in [9] to mobilize the impaired foot with a single DOF device, while the MecDEAR [10] achieved position tracking by a proportional-derivative (PD) controller. An interaction controller was also constructed for ARBOT [2], where the passive training is achieved by a proportional-derivative-integral (PID) controller and a high-level admittance controller processes active training. However, the above mentioned control methods are not implementable for CARR. The complicate nonlinear relationship between contraction force, length and internal pressure of PM makes the linear based method in [11] and the standard PD or PID controller in [10] and [2] have limited performance.

Considering the modeling difficulty of CARR and the repetitive nature of passive ROM training, iterative learning control (ILC) shows great potential. ILC is a typical model-free method for repetitive control object which merely relies on system I/O information and improves the tracking performance gradually [12]. However, studies of ILC on rehabilitation robot are rare. ILC-driven functional electrical stimulation (FES) have been proposed in [13]. Nevertheless, the proposed ILC works as a "high-level" controller to adjust the magnitude of FES while the actual position control was achieved by a PID controller. Conventional PID-type ILC has been applied on several rehabilitation devices because of its simple structure and little calculation burden. A P-type ILC (P-ILC) based feedforward controller has been proposed in [14], and two motor-driven rehabilitation robots [15], [16] achieved multi-joint trajectory tracking by PID-type ILC. However, such contraction mapping based ILC causes unstable transient performance of the system output along iteration domain, meanwhile, the fixed controller structure with unchanged learning gain also degrades the control performance consequently [17].

Inspired by recent works on model-free adaptive control

Manuscript received: Sep 29, 2022; Accepted: Dec 29, 2022. This paper was recommended for publication by Editor Valdastri, Pietro upon evaluation of the Associate Editor and Reviewers' comments.

This work was supported in part by U.K. EPSRC under Grant EP/S019219/1 and Grant EP/V057782/1. (Corresponding authors: Zhenhong Li; Sheng Quan Xie.)

K. Qian, Z. Li, Z. Zhang and S. Q. Xie are with the School of Electronic and Electrical Engineering, Faculty of Engineering, University of Leeds, Leeds LS2 9JT, U.K. (e-mail: el14kq@leeds.ac.uk; Z.H.Li@leeds.ac.uk; Z.Zhang3@leeds.ac.uk; s.q.xie@leeds.ac.uk).

G. Li is with the School of Rehabilitation Medicine, Binzhou Medical University, Yantai 264100, China (e-mail: lgq100@bzmc.edu.cn).

Digital Object Identifier (DOI): see top of this page.

[18], this paper introduces a compact form dynamic linearization (CFDL) technique in iteration domain. Instead of realizing the nonlinear model of PM, the CFDL builds an equivalent data model by using an iteration-dependent time-varying parameter called pseudo partial derivative (PPD). Since PPD is unknown, a data-driven adaptive iterative learning control (DDAILC) algorithm is proposed to estimate the PPD merely using the output measures of the position information. Mathematical analysis is given to guarantee the convergence of algorithm along the iteration domain and bounded-input bounded-output stability along the time domain. Experimental studies are conducted on the CARR for repetitive ROM training with human participants involved. To evaluate the tracking performance of the DDAILC, the comparisons with P-ILC and PID controllers are given.

The main contributions of this work are listed as follows. Instead of modeling the nonlinear PM dynamic, an equivalent data model is established with reasonable assumptions. Only the position measures of the CARR are required to estimate the PPD and design controller. As a nonlinear control algorithm, the development of the DDAILC on the CARR is the first attempt that applying data-driven learning method to the compliant actuator driven device. To mimic the rehabilitation environment, two therapist-resembled trajectories are tested with ten human participants involved. Compared to existing methods, the DDAILC has significant improvement on the tracking performance.

The rest of this paper is arranged as follows. Section II introduces the CARR and formulates the problem. Controller design and convergence analysis are given in Section III. Experimental protocol, results and discussions are presented in Section IV, V and VI with conclusion in Section VII.

II. Preliminaries and Problem Formulation

A. PM-driven CARR and Kinematic Geometry

The concept design of the CARR is shown in Figure 1 (a). It is actuated by four parallel PM actuators with three rotational DOFs for ankle plantarflexion/dorsiflexion (DP), inversion/eversion (IE) and adduction/abduction (AA), which normally denotes as Euler X-, Y- and Z-axis respectively. Each PM actuator is controlled by an independent proportional pressure regulator (PPR). As shown in Figure 1 (b), three rotary encoders are installed to measure angular displacement and a six-axis load cell is installed to measure interaction torque. An embedded controller is adopted to achieve real-time control and three independent data acquisition modules are used for digital I/O, analog input and analog output, respectively. The control interface is developed on a host computer based on LabVIEW and communicates with the embedded controller through TCP/IP protocol.

The inverse kinematics of CARR can be easily obtained and provides a unique solution of the length of PMs for a given end effector posture. Details can be found in our previous work [6]. The length variation caused by compressed air provides actuation of PMs. In consequence, for the PM trajectory tracking control, the internal pressure and length are considered as control input and output respectively.

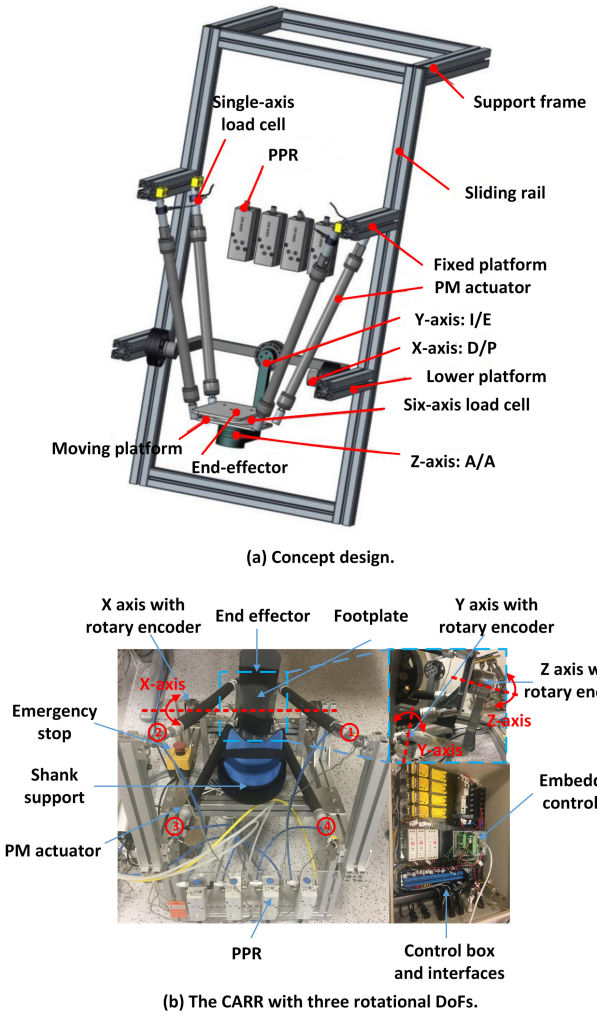

Figure 1: Configurations of the CARR. (a) Concept design. (b) Physical layout of the CARR with three rotational DoFs.

B. Problem Formulation

Four individual PM lengths l_i (index $i = 1, 2, 3, 4$) can be obtained via inverse kinematic [6]. Denote $p_{i,k}(t)$, $l_{i,k}(t) \in \mathbb{R}$ as the input pressure and output length of i-th PM at time instant t during k-th iteration, where $t \in \{0, 1, 2, \ldots, N\}$, $N \in \mathbb{Z}^+$and $k = 1, 2, \cdots$. For an iteration invariant desired trajectory $l_i^*(t)$, the tracking error is defined as $e_{i,k-1}(t+1) = l_i^*(t) - l_{i,k-1}(t+1)$. The main objective of this paper is to find a pressure sequence $p_{i,k}(t)$, such that $e_{i,k-1}(t+1) \to 0$ for $t \in \{0, 1, 2, \ldots, N\}$ as $k \to \infty$. The following discrete-time model is constructed for each PM

$$l_{i,k}(t+1) = f\big(l_{i,k}(t), \ldots, l_{i,k}(t-n_l), p_{i,k}(t), ..., p_{i,k}(t-n_p)\big) \quad (1)$$

where $f(\cdots) : \mathbb{R}^{n_l+n_p+2} \to \mathbb{R}$ is an unknown nonlinear function. $n_l \in \mathbb{Z}^+$ and $n_p \in \mathbb{Z}^+$ are two unknown orders of output $l_{i,k}(t)$ and input $p_{i,k}(t+1)$, respectively.

Assumption 1. *The partial derivative of $f(\cdots)$ with respect to the $(n_l + 2)$ th output variable is continuous.*

Assumption 2. *System (1) satisfies the generalized Lipschitz condition along the iteration domain, that is,* $\forall t = 0, 1, 2, \ldots, N$, $|\Delta l_{i,k}(t+1)| \leq b|\Delta p_{i,k}(t)|$ *for each fixed* k *and* $|\Delta p_{i,k}(t)| \neq 0$, *where* $\Delta l_{i,k}(t+1) = l_{i,k}(t+1) - l_{i,k-1}(t+1), \Delta p_{i,k}(t) = p_{i,k}(t) - p_{i,k-1}(t)$ *and* b *is a positive constant.*

Remark 1. *The Assumptions 1 and 2 imposed on system (1) are easy to satisfy. The Assumption 1 holds if the internal pressure of PM is continuous, the length variation of PM is also continuous. The Assumption 2 is a physical constraint by the inherent nature of PM, i.e., finite change of internal pressure would not lead to infinite change of length.*

Lemma 1. [17] *Suppose Assumptions 1 and 2 hold, for any* $|\Delta p_{i,k}(t)| \neq 0$, *there must exist an iteration-dependent time-varying parameter* $\Phi_{i,k}(t) \in R$, *called pseudo partial derivative (PPD), such that the system (1) can be transformed into the following compact form dynamic linearization (CFDL) data model*

$$\Delta l_{i,k}(t+1) = \Phi_{i,k}(t)\Delta p_{i,k}(t), \quad \forall t \in 0, 1, 2, \cdots, N, \quad \forall k = 1, 2, \cdots \tag{2}$$

with bounded $|\Phi_{i,k}(t)| \leq b$ *for any* t *and* k.

III. Data-driven adaptive ILC and convergence analysis

A. DDAILC Design

Consider the following objective function of the internal pressure $p_{i,k}(t)$

$$J\big(p_{i,k}(t)\big) = |l_i^*(t) - l_{i,k}(t+1)|^2 + \lambda|p_{i,k}(t) - p_{i,k-1}(t)|^2 \tag{3}$$

where $\lambda > 0$ is a weighting factor. Rewriting (2) as

$$l_{i,k}(t+1) = l_{i,k-1}(t+1) + \Phi_{i,k}(t)\Delta p_{i,k}(t). \tag{4}$$

From (4) and the definition of $e_{i,k-1}(t+1)$, Equation (3) can be rewritten as

$$J\big(p_{i,k}(t)\big) = |e_{i,k-1}(t+1) - \Phi_{i,k}(t)\Delta p_{i,k}(t)|^2 + \lambda|\Delta p_{i,k}(t)|^2. \tag{5}$$

Differentiating (5) with respect to $p_{i,k}(t)$, and setting $\frac{\partial J}{\partial p_{i,k}(t)} = 0$, we have

$$\Phi_{i,k}(t)e_{i,k-1}(t+1) = |\Phi_{i,k}(t)|^2\Delta p_{i,k}(t) + \lambda\Delta p_{i,k}(t). \tag{6}$$

Thus, the DDAILC at the k-th iteration is constructed

$$p_{i,k}(t) = p_{i,k-1}(t) + \frac{\rho\,\Phi_{i,k}(t)}{\lambda + |\Phi_{i,k}(t)|^2}e_{i,k-1}(t+1) \tag{7}$$

where $\rho \in (0, 1]$ is a step factor to make the control algorithm more general and related to the convergence properties.

Remark 2. *The* $\Phi_{i,k}(t)$ *is an iteration-dependent time-varying parameter, guaranteeing the algorithm convergence along the iteration domain. The non-causal term* $e_{i,k-1}(t+1)$ *can be obtained from last iteration, which guarantees the stability of the algorithm along time domain within the current iteration.*

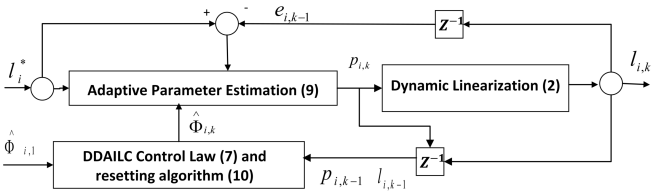

Figure 2: Control diagram of DDAILC for single PM actuator.

Remark 3. *Let* $\Phi_{i,k}(t) = \Gamma_P$, *where* Γ_P *is a positive constant, the control law (7) becomes a traditional P-ILC law with fixed learning gain. The tracking performance of P-ILC will be compared with the proposed DDAILC in Section V.*

Since $\Phi_{i,k}(t)$ is unknown, an estimation algorithm is then constructed for iteratively updating its estimated value $\hat{\Phi}_{i,k}(t)$. Consider the following objective function of $\hat{\Phi}_{i,k}(t)$,

$$J\big(\hat{\Phi}_{i,k}(t)\big) = |\Delta l_{i,k-1}(t+1) - \hat{\Phi}_{i,k}(t)\Delta p_{i,k-1}(t)|^2 + \mu|\hat{\Phi}_{i,k}(t) - \hat{\Phi}_{i,k-1}(t)|^2 \tag{8}$$

where $\mu > 0$ is a weighting factor. Differentiating (8) with respect to $\hat{\Phi}_{i,k}(t)$, and setting $\frac{\partial J}{\partial \hat{\Phi}_{i,k}(t)} = 0$, we have the following $\Phi_{i,k}(t)$ estimation algorithm

$$\hat{\Phi}_{i,k}(t) = \hat{\Phi}_{i,k-1}(t) + \frac{\eta\Delta p_{i,k-1}(t)}{\mu + |\Delta p_{i,k-1}(t)|^2} \times \big(\Delta l_{i_k-1}(t+1) - \hat{\Phi}_{i,k}(t)\Delta p_{i,k-1}(t)\big) \tag{9}$$

where $\eta \in (0, 1]$ is a step factor, being included to make the estimation algorithm more general and flexible.
To strengthen the tracking ability of the estimation algorithm (9), the following reset algorithm is presented

$$\hat{\Phi}_{i,k}(t) = \hat{\Phi}_{i,1}(t), \text{if } |\hat{\Phi}_{i,k}(t)| \leq \varepsilon \text{ or } |\Delta p_{i,k-1}(t)| \leq \varepsilon \text{ or } \operatorname{sign}\big(\hat{\Phi}_{i,k}(t)\big) \neq \operatorname{sign}\big(\hat{\Phi}_{i,1}(t)\big) \tag{10}$$

where $\hat{\Phi}_{i,1}(t)$ is the initial value of $\hat{\Phi}_{i,k}(t)$, ε is a small positive constant. Integrating the control algorithm (7) and parameter estimation algorithm (9) with reset scheme (10), the overall DDAILC for the PM length tracking is constructed, as shown in Figure 2.

B. Convergence Analysis

Assumption 3. *The* $\Phi_{i,k}(t)$ *satisfies that* $\Phi_{i,k}(t) > \sigma > 0, \forall t \in \{0, 1, 2, \cdots, N\}$ *and* $\forall k = 1, 2, \cdots$, *where* σ *is a positive constant.*

Remark 4. *Assumption 3 indicates that the contractile length of PM does not decreases as the corresponding internal pressure increases. Such linear-like characteristic is commonly applied on PM controller design [19].*

Theorem 1. *Suppose Assumptions 1-3 hold for (1). With bounded initial error* $e_{i,1}(t)$ *and initial pressure* $p_{i,1}(t)$, *if the DDAILC controller (7), (9) and (10) are applied and select the weighting factor* $\lambda > \frac{b^2}{4}$, *the following results hold.*
1) Estimated PPD $\hat{\Phi}_{i,k}(t)$ *is bounded.*

2) Tracking error $e_{i,k-1}(t+1)$ monotonically converge to zero.
3) Input pressure $p_{i,k}(t)$ and output $l_{i,k}(t)$ are bounded.

Proof: 1) The boundedness of $\hat{\Phi}_{i,k}(t)$.

For any $|\hat{\Phi}_{i,k}(t)| \leq \varepsilon$ or $|\Delta p_{i,k-1}(t)| \leq \varepsilon$ or $\operatorname{sign}\big(\hat{\Phi}_{i,k}(t)\big) \neq \operatorname{sign}(\hat{\Phi}_{i,1}(t))$, the boundedness of $\hat{\Phi}_{i,k}(t)$ is obvious. Otherwise, define the estimation error $\tilde{\Phi}_{i,k}(t) = \hat{\Phi}_{i,k}(t) - \Phi_{i,k}(t)$. Subtracting $\Phi_{i,k}(t)$ from both side of (9) and substituting (2), we have

$$\begin{aligned}\tilde{\Phi}_{i,k}(t) =&(1 - \frac{\eta|\Delta p_{i,k-1}(t)|^2}{\mu + |\Delta p_{i,k-1}(t)|^2})\tilde{\Phi}_{i,k-1}(t)\\ &- \big(\Phi_{i,k}(t) - \Phi_{i,k-1}(t)\big).\end{aligned} \tag{11}$$

Since $\eta \in (0, 1]$ and $\mu > 0$, the function $\frac{\eta|\Delta p_{i,k-1}(t)|^2}{\mu+|\Delta p_{i,k-1}(t)|^2}$ is monotonically increasing with respect of $|\Delta p_{i,k-1}(t)|^2$. Thus, there exists a positive constant d_1 such that

$$1 - \frac{\eta|\Delta p_{i,k-1}(t)|^2}{\mu + |\Delta p_{i,k-1}(t)|^2} \leq (1 - \frac{\eta\varepsilon^2}{\mu + \varepsilon^2}) = d_1 < 1. \tag{12}$$

Substituting (12) into (11) and take absolute value on both sides, we have

$$|\tilde{\Phi}_{i,k}(t)| \leq d_1|\tilde{\Phi}_{i,k-1}(t)| + 2b \leq d_1^{k-1}|\tilde{\Phi}_{i,1}(t)| + \frac{2b}{1-d_1}. \tag{13}$$

From Lemma 1, $|\Phi_{i,k}(t)| \leq b$ leads to $|\Phi_{i,k}(t) - \Phi_{i,k-1}(t)| \leq 2b$. Thus, $\tilde{\Phi}_{i,k}(t)$ is bounded which implies that $\hat{\Phi}_{i,k}(t)$ is also bounded.

2) The convergence of $e_{i,k}(t+1)$.

By Lemma 1 and (7), we have

$$\begin{aligned}e_{i,k}(t+1) =&l_{i,d}(t+1) - l_{i,k}(t+1) -\\ &\hat{\Phi}_{i,k}(t)|p_{i,k}(t) - p_{i,k-1}(t)|\\ =&\big(1 - \frac{\rho\Phi_{i,k}(t)\hat{\Phi}_{i,k}(t)}{\lambda + |\hat{\Phi}_{i,k}(t)|^2}\big)e_{i,k-1}(t+1).\end{aligned} \tag{14}$$

Since $\lambda + |\hat{\Phi}_{i,k}(t)|^2 \geq 2\sqrt{\lambda}\hat{\Phi}_{i,k}(t)$ and $\Phi_{i,k}(t)$ is bounded by b, there must exist a positive constant d_2 such that

$$0 < d_2 \leq \frac{\Phi_{i,k}(t)\hat{\Phi}_{i,k}(t)}{\lambda + |\hat{\Phi}_{i,k}(t)|^2} \leq \frac{b}{2\sqrt{\lambda}}. \tag{15}$$

Since $\rho \in (0, 1]$ and $\lambda > \frac{b^2}{4}$, according to (15), there must exist a positive constant $d_3 < 1$ such that

$$\begin{aligned}&0 < d_2 \leq \frac{b}{2\sqrt{\lambda}} < 1 \quad \text{and}\\ &|1 - \frac{\rho\Phi_{i,k}(t)\hat{\Phi}_{i,k}(t)}{\lambda + |\hat{\Phi}_{i,k}(t)|^2}| \leq 1 - \rho d_2 \triangleq d_3 < 1.\end{aligned} \tag{16}$$

Taking absolute value on both sides of (14) and using (16), we have

$$\begin{aligned}|e_{i,k}(t+1)| &= |1 - \frac{\rho\Phi_{i,k}(t)\hat{\Phi}_{i,k}(t)}{\lambda + |\hat{\Phi}_{i,k}(t)|^2}||e_{i,k-1}(t+1)|\\ &\leq d_3|e_{i,k-1}(t+1)|\\ &\vdots\\ &\leq d_3^{k-1}|e_{i,1}(t+1)|.\end{aligned} \tag{17}$$

which indicates that $e_{i,k}(t+1)$ converges to zero in a pointwise manner over the finite time interval N when $k \to \infty$.

3) The boundedness of $l_{i,k}(t)$ and $p_{i,k}(t)$.

Since $l_i^*(t)$ is iteration-invariant, the convergence of $e_{i,k}(t)$ implies that $l_{i,k}(t)$ is also bounded. Using same procedure in (16), we have

$$\begin{aligned}|\Delta p_{i,k}(t)| &= \left|\frac{\rho\hat{\Phi}_{i,k}(t)e_{i,k-1}(t+1)}{\lambda + |\hat{\Phi}_{i,k}(t)|^2}\right|\\ &\leq \left|\frac{\rho}{2\sqrt{\lambda_{min}}}\right||e_{i,k-1}(t+1)|\\ &\triangleq d_4|e_{i,k-1}(t+1)|\end{aligned} \tag{18}$$

where d_4 is a bounded positive constant.

Expanding $p_{i,k}(t)$ into following form

$$\begin{aligned}|p_{i,k}(t)| =&|p_{i,k}(t) - p_{i,k-1}(t)| + |p_{i,k-1}(t) - p_{i,k-2}(t)| + \cdots\\ &+ |p_{i,2}(t) - p_{i,1}(t)| + |p_{i,1}(t)|\\ =&|\Delta p_{i,k}(t)| + \cdots + |\Delta p_{i,2}(t)| + |p_{i,1}(t)|.\end{aligned} \tag{19}$$

According to (17), (18) and (19), we have

$$|p_{i,k}(t)| \leq d_4\frac{1}{1-d_3}|e_{i,1}(t+1)| + |p_{i,1}(t)|. \tag{20}$$

Since both initial error and pressure are given bounded, the equation (20) implies that $p_{i,k}(t)$ is bounded $\forall t \in \{0, 1, 2, \cdots, N\}$ and $\forall k = 1, 2, \cdots$. ■

IV. Subjects and Experimental Protocol

The feasibility of DDAILC is first tested on the CARR without human participants. Subsequently, passive training are performed on ten healthy subjects (P1-P10 for short) with no neurological injury or recent physical ankle impairment. This trial has been approved by the University of Leeds Research Ethics Committee (reference MEEC 18-001). Desired trajectories are selected as sinusoidal waveforms with $t = 0.05\,\mathrm{s}$. The maximum ROM is $0.3\,\mathrm{rad}$ and the movement period is $20\,\mathrm{s}$. During training, subjects are asked to adjust the sitting posture such that their ankles are fully relaxed. To imitate physical rehabilitation procedure, two therapist-resembled movements [20] are suggested by the therapist:

T1: Joint movement along both X and Y-axis which from neutral position to $0.2\,\mathrm{rad}$ dorsiflexion/inversion and $0.2\,\mathrm{rad}$ plantarflexion/eversion.

T2: First trial with $0.2\,\mathrm{rad}$ amplitude along X-axis and progressive training increases the amplitude to $0.3\,\mathrm{rad}$.

The commonly used PID controller in compliant actuator driven device [21–23] and P-ILC are implemented for comparison. Table I summarizes the well-tuned control parameters.

Table I: Designed control parameters.

Controller	Control parameters
PID	$K_p = 20$, $K_i = 9 \times 10^{-3}$, $K_d = 2.25 \times 10^{-3}$
P-ILC	$\Gamma_p = 0.8$
DDAILC	$\rho = 1, \lambda = 1.5, \mu = 1$, $\eta = 0.2$, $\hat{\Phi}_{i,1}(t) = 2$

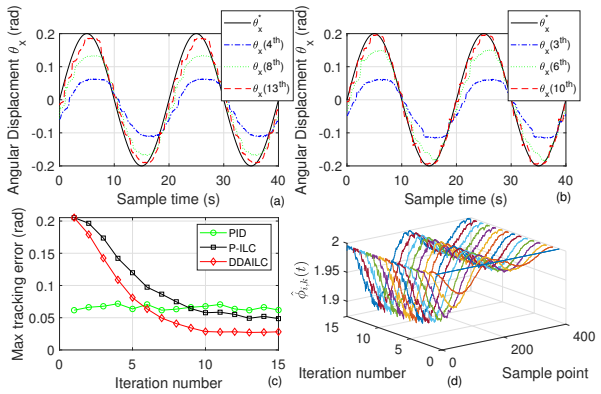

Figure 3: Tracking results along X-axis. (a) P-ILC. (b) Proposed DDAILC. (c) Maximum error convergence. (d) The $\hat{\phi}_{i,k}(t)$ of PM1 along both domains.

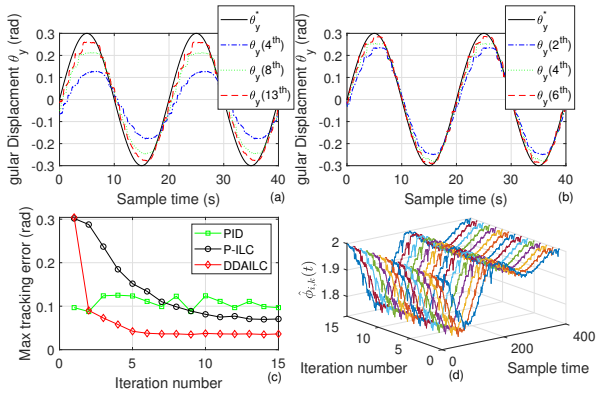

Figure 4: Tracking results along Y-axis (0.3 rad). (a) P-ILC. (b) Proposed DDAILC. (c) Maximum error convergence. (d) The $\hat{\phi}_{i,k}(t)$ of PM1 along both domains.

V. Results

A. Repetitive CARR Control

A sinusoidal trajectory along X-axis with 0.2 rad amplitude is adopted first and ILC methods can gradually reduce the tracking error, as shown in Figure 3(a) and (b). From error convergence curves in Figure 3(c), the PID maintains a maximum 0.06 rad tracking error. The P-ILC and DDAILC requires 10 and 6 iterations to achieve a maximum tracking error of 0.05 rad and 0.03 rad, respectively. The value of $\hat{\Phi}_{i,k}(t)$ is given in Figure 3(d) which updates in the learning stage and maintains similar curve when the tracking error is converged.

Conducting different DoFs and ROMs training are essential in the rehabilitation scenario. In virtue of its data-driven nature, DDAILC is expected to adapt different trajectories. Therefore, a sinusoidal trajectory with 0.2 rad amplitude is conducted along Y-axis for 15 iterations, consequently, 15 more iterations are performed that increase the amplitude to 0.3 rad. Note that designed control parameters are remain unchanged to eliminate the effects of controller tuning.

Tracking performances of the last 15 iterations are shown in Figure 4. The P-ILC starts a new learning progress ($p_{i,1}(t) = 0$) and requires 13 iterations for an error convergence of 0.07 rad. Although the pressure is initialized, DDAILC can use the stored value of $\hat{\Phi}_{i,k}(t)$ that provides an equivalent pressure sequence which drive the CARR to a 0.2 rad trajectory, as illustrated in Figure 4(c). Subsequently, only 4 more iterations are required for a 0.035 rad error. It can be also observed in Figure 4(d) that the stored value of $\hat{\Phi}_{i,k}(t)$ effectively works in the first iteration.

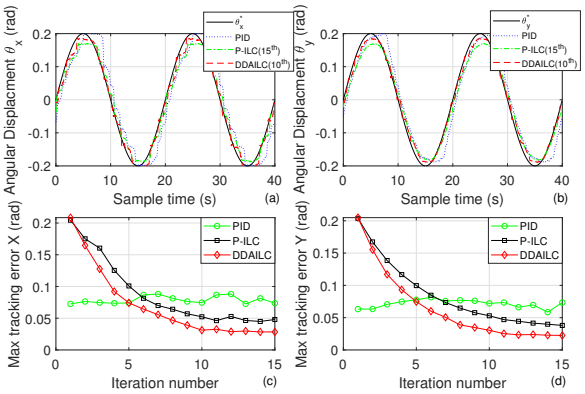

Figure 5: Tracking results of T1. (a) X-axis. (b) Y-axis. (c) X-axis error convergence. (d) Y-axis error convergence.

B. Passive Training with Human Participants

Although participants are encouraged to keep ankle joint relaxed, the individual passive torque produced by the stretching of muscles, tendons and ligaments is inevitable. This passive torque is not considered in our controller design, which can evaluate the performance of DDAILC with uncertainties. In our previous work [24], the PM length tracking was studied along a vertical direction and control performance with such uncertainties have not been validated. In this section, the tracking performances of different controllers under T1 and T2 are compared and participants' passive torque are discussed. Tracking performances of P1 are chosen as an example and presented in Figure 5 and 7, respectively. Detailed working conditions of PMs including individual muscle length convergences and the objective functions $J\big(p_{i,k}(t)\big)$ are given in Figure 6 and 8. The green, black, red and blue lines represent PM1-PM4 as shown in Figure 1. The passive torque of P1 and P2 and the tracking performances are detailed in Figure 9.

The tracking results and error convergence along different axes of T1 are given in Figures 5. Without any parameters change, the DDAILC converges the tracking error to 0.03 rad and 0.025 rad after 10 iterations. Although the P-ILC follows the trajectory after 15 iterations, 5% and 10% increases of tracking error along X and Y-axis are found when compared to non-participant results. Moreover, the performance of PID becomes worse where the tracking error for both axes have increased 0.02 rad.

Detailed working conditions of individual PMs are presented in Figure 6. Due to the different length of contraction, Figure 6(a) demonstrates that PM2 and PM4 have larger control range with a 4 mm tracking error, while PM1 and PM3 converge the error to 2 mm. Same conditions can be found in Figure 6(b), where PM2 and PM4 decrease the value of

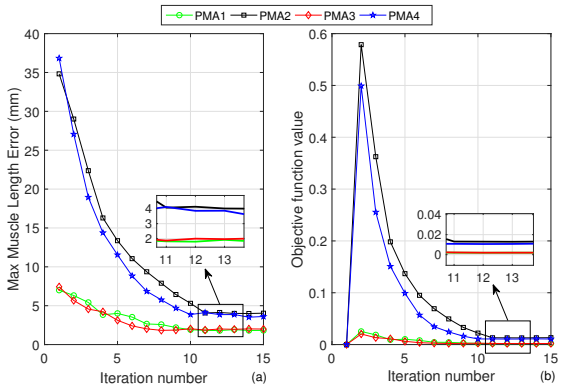

Figure 6: Muscle length convergences and objective functions of T1. (a) Muscle length convergences. (b) The $J\big(p_{i,k}(t)\big)$.

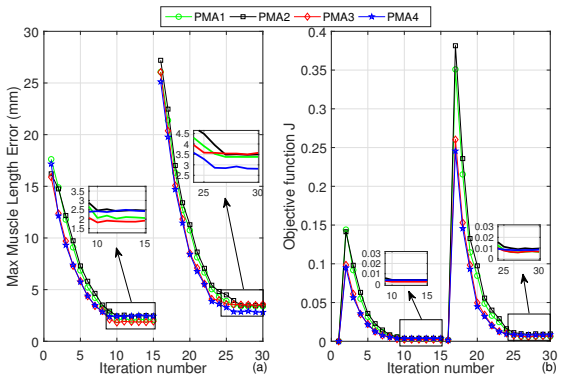

Figure 8: Muscle length convergences and objective functions of T2. (a) Muscle length convergences. (b) The $J\big(p_{i,k}(t)\big)$.

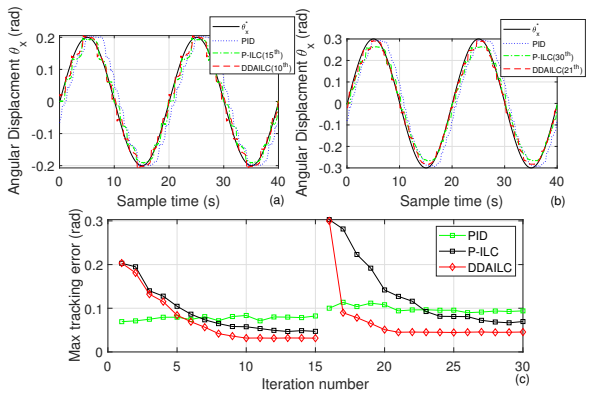

Figure 7: Tracking results of T2. (a) First trail. (b) Follow-up trail. (c) Overall convergence curve along two trails.

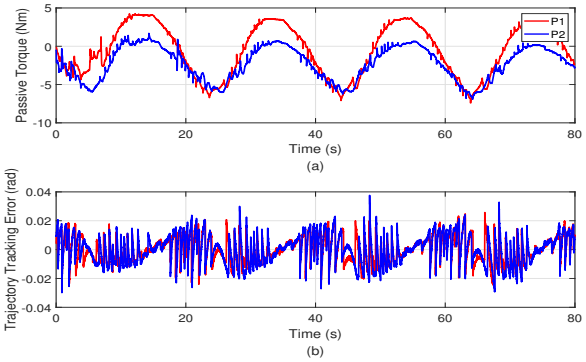

Figure 9: Passive ankle torque and trajectory tracking error of the DDAILC after 10 iterations. (a) Passive torque. (b) Tracking error.

$J\big(p_{i,k}(t)\big)$ from over 0.5 to 0.01 while PM1 and PM3 converge it from 0.03 to 0.002.

Tracking performances of different controllers under T2 are presented in Figure 7. With the readable value of $\hat{\Phi}_{i,k}(t)$, the convergence speed of DDAILC for the progressive trajectory has greatly improved. From Figure 7(c), we can observe that the P-ILC and PID both have significant increase on maximum tracking error when the control range is increased. The PID has an increase of tracking error from $0.08\,\mathrm{rad}$ to $0.1\,\mathrm{rad}$ and the P-ILC reduces it to $0.06\,\mathrm{rad}$. However, the DDAILC shows significant improvement with a tracking error under $0.04\,\mathrm{rad}$.

The different dynamics of PMs under T2 can be clearly observed in Figure 7(a). The maximum length error of four PMs are around $2\,\mathrm{mm}$ for the first trail and $3.5\,\mathrm{mm}$ for the progressive training. After the initial setting at 1^{th} and 16^{th} iteration as shown in Figure 8(b), the values of $J(p_{i,k}(t))$ for both trail are started from 0.15 and 0.38 and converges to 0.005 and 0.01.

The PM is backdrivable due to its inherent compliance, which makes it safer to drive when encountered with joint resistance torque. However, the nonlinear dynamics and time-varying property bring difficulties to precise trajectory tracking control. Figure 9 illustrates the passive ankle torque and tracking performance of P1 and P2 after 10 training iterations. Due to personal differences, we observe in Figure 9(a) that P1 has a larger passive plantarflexion torque than P2, i.e., P1 has a higher ankle stiffness than P2. Despite the difference in ankle stiffness, the DDAILC is able to maintain a sufficiently small tracking error, as shown in Figure 9(b).

To statistically analyze the tracking performance of different controllers, three criteria are analyzed and calculated by

$$\mathrm{RMSE} = \sqrt{\frac{\sum_{t=1}^{N}\big(\theta^*(t) - \theta_{15}(t)\big)^2}{N}} \tag{21}$$

$$\text{Peak error (PE)} = \frac{\sum|\theta^*(t) - \theta_{15}(t)|}{2},\ t = 100, 300 \tag{22}$$

$$\text{Maximum error (ME)} = \mathrm{Max}(|\theta^*(t) - \theta_{15}(t)|) \tag{23}$$

where $\mathrm{Max}(\cdot)$ returns the largest value for $t \in N$. Statistical analysis results of ten subjects are shown in Table II and Figure 9 where the conventional P-ILC has improvements on RMSE and ME when compared to the PID controller. With the introduction of $\Phi_{i,k}(t)$, both criteria have further improved by the DDAILC. For the PE, the P-ILC performs closely or even worse than the PID controller. It intuitively demonstrates the major drawback of the conventional P-ILC, i.e., the performance degradation during later period of learning. On the contrary, with the iteration-dependent time-varying $\Phi_{i,k}(t)$, DDAILC alleviates this drawback and provides effective error

Table II: The statistical results of three performance criteria for T1 and T2.

		RMSE (rad)			PE (rad)			ME (rad)		
T1	Trail number	5	10	15	5	10	15	5	10	15
P-ILC	X-axis	0.0607	0.0274	0.0215	0.0873	0.0327	0.0252	0.1027	0.059	0.05
	Y-axis	0.0594	0.0289	0.0217	0.0852	0.0402	0.0272	0.0968	0.0503	0.0374
DDAILC	X-axis	0.045	0.0155	0.0117	0.0663	0.0184	0.0063	0.0837	0.0375	0.0272
	Y-axis	0.0429	0.0121	0.0087	0.0649	0.0157	0.0085	0.0719	0.0293	0.0185
PID	X-axis	0.0403			0.0171			0.0898		
	Y-axis	0.0353			0.0169			0.0724		

T2	Amplitude	0.2 rad		0.3 rad		0.2 rad		0.3 rad		0.2 rad		0.3 rad	
	& Trail number	5	15	5	15	5	15	5	15	5	15	5	15
P-ILC	X-axis	0.061	0.0201	0.0918	0.0305	0.0767	0.0104	0.1253	0.0345	0.1004	0.0493	0.1509	0.065
DDAILC	X-axis	0.0463	0.0128	0.0157	0.0129	0.0627	0.005	0.0101	0.0046	0.0862	0.0299	0.052	0.0444
PID	X-axis	0.0471		0.0592		0.011		0.0216		0.0915		0.1122	

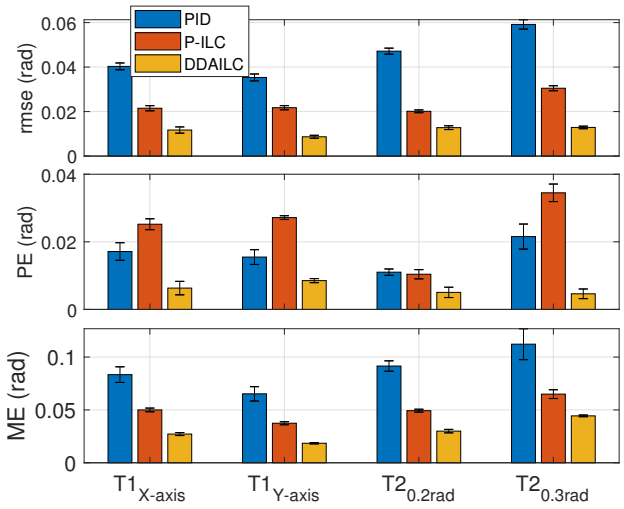

Figure 10: Statistical analysis of different controllers. From top to bottom: RMSE, PE and ME. Colored bars represent the mean value and error bars denote the standard error.

compensation with a PE under 0.007 rad.

To further validate the performance of DDAILC, a comparison is made with published control schemes for conducting the CARR trajectory tracking [6, 25–27]. In addition to the data-driven tuning method [6], analytical PM model is required for designing the position-force control scheme [25], sliding mode controller [26] and inverse model-based ILC [27]. Due to the difference of the predefined trajectory, tracking performance is normalized to maximum error percentage in total movement range as shown in Table III. It can be seen that, the tracking performance of data-driven controllers outperform other methods, meanwhile, DDAILC has a significant improvement over the conventional P-ILC. Considering the repetitive rehabilitation scenario, the performance of DDAILC and its feasibility in conducting ROM training are further demonstrated.

VI. Discussion

The prolonged immobility of stroke survivors during their acute period will worsen muscle weakness and joint contractures. Conducting passive training by completing a ROM trajectory has shown to be effective in relieving these symptoms [9]. Moreover, ankle stretching can effectively reduce the joint

Table III: Comparison with trajectory tracking studies for PM-driven robots.

Control strategy	Performance*	Reference
The proposed DDAILC	9.25%	-
The applied P-ILC	18.7%	-
Robust IFT tuning	17.44%	[6]
Hierarchical force-position	20.8%	[25]
SMC with boundary layer	25.7%	[26]
Inverse model-based ILC	21.3%	[27]

* ME percentage in total movement range.

stiffness and decrease the incidence of muscle strain during subsequent training sessions [28, 29]. As a typical repetitive scenario, the automation capability of robotic sustains its potential in joint stretching and passive ROM training. From a control prospective, repetitiveness provides the task domain for implementing the learning-based methods on the CARR, e.g., the conventional ILC [14–16]. However, the strong nonlinearity of PM and the time-varying property of human subject limit its tracking performance which results in inadequate training outcomes. Considering the performance degradation with the fixed control structure, adaptive ILC scheme and parameter estimation algorithm are designed in this paper, as shown in (7) and (9). Moreover, to resolve the unstable transient behavior caused by asymptotic convergence, sufficient conditions are given that guarantee monotonic convergence of the robot tracking error, as proven in Theorem 1.

Unlike prototype developed in [2, 3, 22], the CARR aligns its rotation center with the ankle joint such that synergistic movements of the user's lower extremity are eliminated. This design is motivated by the clinical outcomes [30], i.e., isolated movements for single-joint are easier to be learned and therefore have less reliance on neural factors than multiple-joint exercises. Compared to an electric motor, PM can deliver compliant actuation and provide extra ROM for the subject's active backdrive. Meanwhile, the passive torque provided by the muscles, tendons and ligaments will bring uncertainties during training. Figure 9 illustrates the personal difference in ankle passive torque caused by different ankle stiffness and validates the tracking performance of the DDAILC. Moreover, the comparison results for the selected controllers under different tasks are summarized in Figure 10. It can be observed

that the standard error of the PID for RMSE, PE and ME are larger than the learning-based approaches, indicating that its control performance is affected by task differences. For the learning-based methods, especially the DDAILC, the standard error is relatively small which guarantees a reliable tracking under different training tasks.

When examining the performance of the proposed control scheme, two movements are adopted under suggestions of the physiotherapist while the DoF along Z-axis is not recommended. Compared to the PID controller, the P-ILC has an improvement on the RMSE (i.e. 51.5%) and ME (i.e. 57.93%) that represents the accuracy and stability of the trajectory tracking. With the proposed DDAILC, these two criteria are further improved by 29.73% and 18.36%. The completion of a prescribed trajectory, i.e., reaching the peak ankle ROM, is significant for improving the training effectiveness [28]. Due to the fixed structure of the controller, the P-ILC is less effective in the late learning period when the error is close to converge. By constricting the $\Phi_{i,k}$ along both time and iteration domains, the peak tracking error of DDAILC was improved by 50.3% when compared to the PID controller.

Although our proposed control scheme has a significant improvement in robot tracking performance, as a trade-off, it requires 8 iterations to converge the tracking error. To adapt a wider range of training requirements, accelerating the convergence speed of ILC-based methods can be considered as the next stage of study. Moreover, implementing an ILC-based compensator alongside a well-tuned feedback controller is also an alternative way for the robot to quickly perform the desired trajectory and gradually enhance its training performance by the learning-based mechanism.

VII. Conclusion

In summary, a data-driven adaptive iterative learning controller is proposed for effective ankle stretching and passive ROM training. The dynamic linearization approach is introduced and the rigorous mathematical proof is given to guarantee the convergence and the boundedness of the algorithm. Two rehabilitation training movements are conducted on ten human participants. Compared to the P-ILC and PID controllers, results show that the proposed DDAILC has significant improvement on the tracking performance which maintain the tracking error under 9%.

References

[1] D. Yoo, Y. Son *et al.*, "Technology-assisted ankle rehabilitation improves balance and gait performance in stroke survivors: a randomized controlled study with 1-month follow-up," *IEEE Trans. Neural Syst. Rehabil. Eng.*, vol. 26, no. 12, pp. 2315–2323, 2018.

[2] J. A. Saglia, N. G. Tsagarakis *et al.*, "Control strategies for patient-assisted training using the ankle rehabilitation robot (ARBOT)," *IEEE/ASME Trans. Mech.*, vol. 18, no. 6, pp. 1799–1808, 2013.

[3] M. Girone, Burdea *et al.*, "A stewart platform-based system for ankle telerehabilitation," *Auton. Robot.*, vol. 10, no. 2, pp. 203–212, 2001.

[4] D. P. Romilly, C. Hershler *et al.*, "A functional task analysis and motion simulation for the development of a powered upper-limb orthosis," *IEEE Trans. Rehabil. Eng.*, vol. 2, no. 3, pp. 119–129, 1994.

[5] J. Cao, S. Q. Xie *et al.*, "MIMO sliding mode controller for gait exoskeleton driven by pneumatic muscles," *IEEE Trans. Control Syst. Technol.*, vol. 26, no. 1, pp. 274–281, 2018.

[6] W. Meng, S. Q. Xie *et al.*, "Robust iterative feedback tuning control of a compliant rehabilitation robot for repetitive ankle training," *IEEE/ASME Trans. Mech.*, vol. 22, no. 1, pp. 173–184, 2017.

[7] C. M. Thalman, M. Debeurre *et al.*, "Entrainment during human locomotion using a soft wearable ankle robot," *IEEE Robot. Autom. Lett.*, vol. 6, no. 3, pp. 4265–4272, 2021.

[8] X. Hu, X. Zeng *et al.*, "A soft robotic intervention for gait enhancement in older adults," *IEEE Trans. Neural Syst. Rehabil. Eng.*, vol. 29, pp. 1838–1847, 2021.

[9] Y. Ren, Y.-N. Wu *et al.*, "Developing a wearable ankle rehabilitation robotic device for in-bed acute stroke rehabilitation," *IEEE Trans. Neural Syst. Rehabil. Eng.*, vol. 25, no. 6, pp. 589–596, 2016.

[10] G. Bucca, A. Bezzolato *et al.*, "A mechatronic device for the rehabilitation of ankle motor function," *J. Biomech. Eng.*, vol. 131, no. 12, p. 125, 2009.

[11] L. Q. Zhang, S. G. Chung *et al.*, "Intelligent stretching of ankle joints with contracture/spasticity," *IEEE Trans. Neural Syst. Rehabil. Eng.*, vol. 10, no. 3, pp. 149–157, 2002.

[12] M. Pierallini, F. Angelini, A. Bicchi, and M. Garabini, "Swing-up of underactuated compliant arms via iterative learning control," *IEEE Robot. Autom. Lett.*, vol. 7, no. 2, pp. 3186–3193, 2022.

[13] C. T. Freeman, Hughes *et al.*, "Iterative learning control of FES applied to the upper extremity for rehabilitation," *Control Eng. Pract.*, vol. 17, no. 3, pp. 368–381, 2009.

[14] S. Balasubramanian, R. Wei *et al.*, "RUPERT: An exoskeleton robot for assisting rehabilitation of arm functions," in *Proc. 2008 Virtual Rehabil. Conf.*, Aug 2008, pp. 163–167.

[15] Q. Miao, H. S. Lo *et al.*, "Iterative learning control method for improving the effectiveness of upper limb rehabilitation," in *Proc. 2016 Int. Conf. on Mech. & Mach. Vis. in Pract.*, Nov 2016, pp. 1–5.

[16] X. Zhu, J. Wang *et al.*, "Nonlinear iterative learning control of 5 dof upper-limb rehabilitation robot," in *IEEE Int. Conf. on Robot. & Biomim.*, Dec 2015, pp. 793–798.

[17] X. Bu, Q. Yu *et al.*, "Model free adaptive iterative learning consensus tracking control for a class of nonlinear multiagent systems," *IEEE Trans. Syst., Man, Cybern., Syst.*, vol. 49, no. 4, pp. 677–686, 2017.

[18] Z. Hou and S. Jin, *Model free adaptive control: theory and applications*. CRC press, 2019.

[19] J. Huang, Y. Cao *et al.*, "An echo state gaussian process-based nonlinear model predictive control for pneumatic muscle actuators," *IEEE Trans. Autom. Sci. Eng.*, vol. 16, no. 3, pp. 1071–1084, 2018.

[20] P. W. Duncan, L. B. Goldstein *et al.*, "Similar motor recovery of upper and lower extremities after stroke." *Stroke*, vol. 25, no. 6, pp. 1181–1188, 1994.

[21] M. Zhang, S. Q. Xie *et al.*, "Adaptive patient-cooperative control of a compliant ankle rehabilitation robot (CARR) with enhanced training safety," *IEEE Trans. Ind. Electron.*, vol. 65, no. 2, pp. 1398–1407, 2017.

[22] A. Roy, H. I. Krebs *et al.*, "Robot-aided neurorehabilitation: a novel robot for ankle rehabilitation," *IEEE Trans. Robot.*, vol. 25, no. 3, pp. 569–582, 2009.

[23] Y. Pan, X. Li *et al.*, "Efficient PID tracking control of robotic manipulators driven by compliant actuators," *IEEE Trans. Control Syst. Technol.*, vol. 27, no. 2, pp. 915–922, 2018.

[24] Q. Ai, Z. Zhang *et al.*, "High-order model-free adaptive iterative learning control of pneumatic artificial muscle with enhanced convergence," *IEEE Trans. Ind. Electron.*, vol. 67, no. 11, pp. 9548–9559, 2020.

[25] Q. Liu, W. Meng *et al.*, "Hierarchical compliance control of a soft ankle rehabilitation robot actuated by pneumatic muscles," *Front. Neurorobotics*, vol. 11, p. 64, 2017.

[26] J. H. Lilly and L. Yang, "Sliding mode tracking for pneumatic muscle actuators in opposing pair configuration," *IEEE Trans. Control Syst. Technol.*, vol. 13, no. 4, pp. 550–558, 2005.

[27] D. H. Owens, C. T. Freeman *et al.*, "An inverse-model approach to multivariable norm optimal iterative learning control with auxiliary optimisation," *Int. J. Control*, vol. 87, no. 8, pp. 1646–1671, 2014.

[28] P. J. McNair, E. W. Dombroski *et al.*, "Stretching at the ankle joint: viscoelastic responses to holds and continuous passive motion," *Med. Sci. Sports Exerc.*, vol. 33, no. 3, pp. 354–358, 2001.

[29] N. Guissard and J. Duchateau, "Neural aspects of muscle stretching," *Exerc. Sport Sci. Rev.*, vol. 34, no. 4, pp. 154–158, 2006.

[30] O. Rutherford and D. Jones, "The role of learning and coordination in strength training," *Eur. J. Appl. Physiol.*, vol. 55, no. 1, pp. 100–105, 1986.